

# 25-GHz Polarization-Insensitive Electroabsorption Modulators with Traveling-Wave Electrodes

Sheng Z. Zhang, Yi-Jen Chiu, Patrick Abraham, and John E. Bowers, *Fellow, IEEE*

**Abstract**— Electroabsorption modulators with traveling-wave electrodes have been designed and fabricated using MOCVD grown InGaAsP–InGaAsP quantum wells. A modulation bandwidth of 25 GHz is achieved for a 2- $\mu\text{m}$ -wide 300- $\mu\text{m}$ -long device. Driving voltage of 1.20 V is achieved for an extinction ratio of 20 dB for operation at 1.55  $\mu\text{m}$ .

**Index Terms**— Electroabsorption, optical fiber communication, optical modulation, quantum-confined Stark effect, quantum-well devices, traveling-wave devices.

## I. INTRODUCTION

ELECTROABSORPTION (EA) modulators are very attractive devices for optical fiber communications because of their very low driving voltage, very high modulation efficiency and integrability with lasers [1]. However, conventional EA modulators are lumped-electrode devices, whose speeds are limited by the total parasitics of the devices, which restricts the devices to very short length for high-speed operation [2]–[4]. One way to overcome the parasitic limitation is by integrating passive waveguides with a short absorption section [2]–[3]. However, this kind of device with short active regions has lower extinction ratio and requires relatively higher driving voltage. On the other hand, a traveling wave electrode structure can overcome the  $RC$  limitation and allows for longer devices for the same speed requirement, which potentially lowers the required driving voltage, increases the extinction ratio and the optical saturation power [5]–[7].

In this letter, we demonstrate 1.55- $\mu\text{m}$  traveling-wave EA modulators (TEAM) fabricated with MOCVD grown InGaAsP–InGaAsP quantum wells. We also examine the effect of load termination on the high-speed performance.

## II. DESIGN AND FABRICATION

A coplanar waveguide (CPW) electrode structure is designed for both the microwave feed line region and the optical waveguide region [7]–[8]. Fig. 1 shows the SEM picture of a 300- $\mu\text{m}$ -long device. The feed line is 500  $\mu\text{m}$  long on each side of the optical waveguide. The ridge is formed by  $\text{CH}_4/\text{H}_2/\text{Ar}$  reactive ion etch (RIE) followed by a  $\text{HCl}:\text{H}_3\text{PO}_4$  wet etch to reduce RIE damage. PMGI is used to passivate the sidewalls and to reduce the capacitance due to the p-electrode on the

Manuscript received August 12, 1998; revised September 18, 1998. This work was supported by the Defense Advanced Research Projects Agency under the Ultra Photonics program.

The authors are with the Department of Electrical and Computer Engineering, University of California at Santa Barbara, Santa Barbara, CA 93106 USA. Publisher Item Identifier S 1041-1135(99)01102-7.

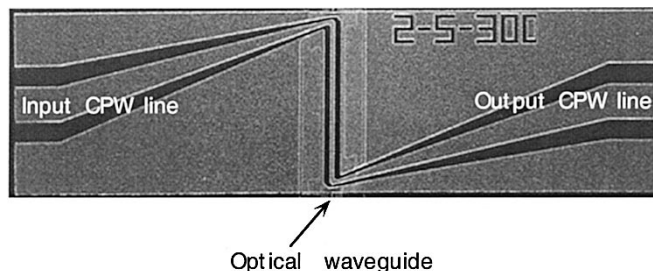


Fig. 1. SEM picture of the top view of a 300- $\mu\text{m}$  traveling-wave EA modulator.

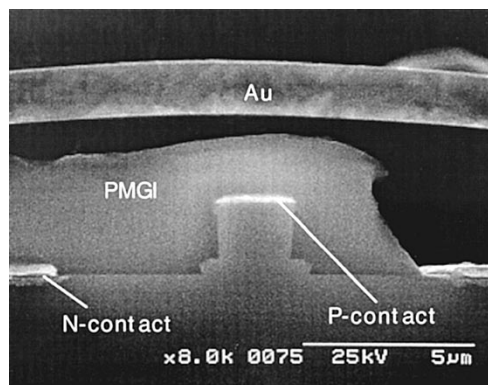


Fig. 2. SEM facet view of a cleaved modulator with a ridge width of 2  $\mu\text{m}$ .

optical waveguide. As shown in the figure, PMGI bridges are formed on both ends of the optical waveguide to connect grounds from different sides of the optical waveguide.

The material structure consists of 0.5- $\mu\text{m}$   $\text{n}^+\text{-InP}$  bottom contact layer, 0.3- $\mu\text{m}$   $\text{n-InP}$  cladding layer, ten strain-compensated InGaAsP quantum well (10.4 nm, 0.37% tensile strain) and InGaAsP barrier (7.6 nm, 0.5% compressive strain), 1.5- $\mu\text{m}$   $\text{p-InP}$  cladding layer and 0.1- $\mu\text{m}$   $\text{p}^+\text{-InGaAs}$  top contact layer on the semi-insulating InP substrate. The material has a room temperature photoluminescence (PL) peak at 1495 nm. Fig. 2 shows the SEM facet view of a cleaved device with a width of 2  $\mu\text{m}$ .

## III. EXPERIMENTAL RESULTS

A lens pair is used to couple light from fiber to the waveguide and vice versa. High-frequency measurements are performed with an HP Lightwave Component Network Analyzer. Two Cascade probes are used for the microwave connection and one of the probes is terminated with a 50- $\Omega$  load.

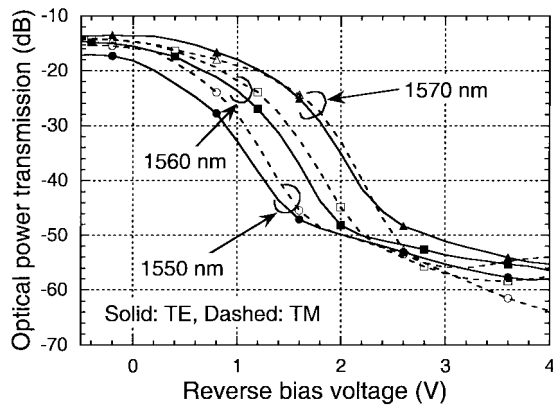


Fig. 3. Fiber-to-fiber transmission versus reverse bias voltage for several wavelengths and for TE and TM polarization states. Solid: TE polarization, Dashed: TM polarization.

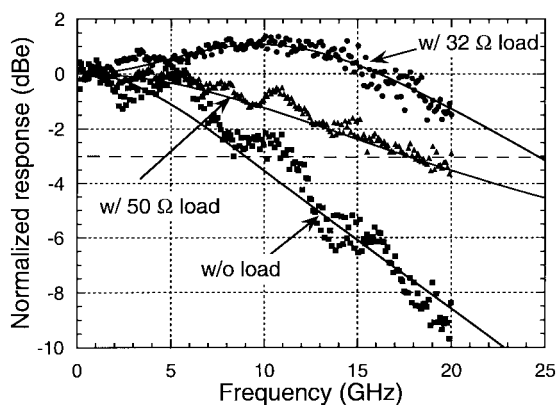


Fig. 4. Measured and simulated EO responses (in dB) for a 2- $\mu\text{m}$  wide 300- $\mu\text{m}$ -long traveling-wave modulator. Curves: Theory. Dots: Measurement.

Fig. 3 shows the fiber-to-fiber transmission versus reverse bias voltage for several wavelengths and for TE and TM polarization states. The device shows little dependence on the polarization, which is a result of proper bandgap engineering. The 2- $\mu\text{m}$ -wide 300- $\mu\text{m}$ -long device has driving voltages of 1.20 and 1.28 V for 20 dB extinction ratio for TE and TM modes respectively at wavelength of 1.55  $\mu\text{m}$ . A fiber-to-fiber insertion loss of 13.6 dB is achieved at 1.57  $\mu\text{m}$  for TM polarization without antireflection coating.

An equivalent circuit model is used to simulate the electrical to optical response performance [8]. Three different cases are compared: 1) no termination, 2) with 50- $\Omega$  termination, and 3) with 32- $\Omega$  termination. The calculated EO responses are shown as lines in Fig. 4.

The frequency responses at three different terminations are measured and shown as dots in Fig. 4. The 32- $\Omega$  termination is achieved by wire bonding a thin-film resistor to the device. With a 50- $\Omega$  termination, a bandwidth of 18 GHz is obtained, yielding a bandwidth to driving voltage (0.8 V for 10-dB extinction) ratio of 22.5 GHz/V. The bandwidth reduces to 10.7 GHz when there is no termination. The reason for this large bandwidth reduction is the large reflection from the unterminated port. The capacitance and the series resistance of the device deduced from the electrical  $S_{11}$  measurement are 0.40 pF and 4.6  $\Omega$ , which infers RC limited bandwidths of 7.3

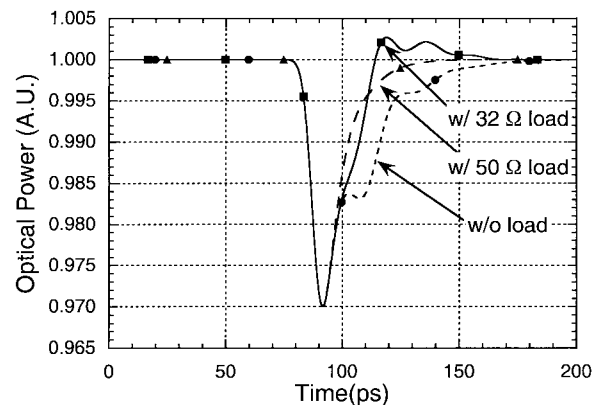


Fig. 5. Simulated optical output under the modulation of a Gaussian pulse.

and 13.4 GHz for cases with and without a 50- $\Omega$  termination. The larger bandwidth for the TEAM than that for the lumped device confirms that traveling-wave electrode structure can overcome the RC limitation.

The bandwidth for the case with a 32- $\Omega$  termination increases to about 24.5 GHz, yielding a bandwidth to driving voltage (0.8 V for 10-dB extinction) ratio of 30.6 GHz/V.

#### IV. DISCUSSION

The key feature on the response curve with 32- $\Omega$  termination is the resonance peak, which is mainly caused by the microwave reflections at the load and the source ends and at the interfaces between the optical waveguide and the feed lines. Because of the negative reflection at the load, the response at some frequencies is enhanced. This can be seen in Fig. 5, which shows the simulated optical signal output under small signal modulation. Here, a Gaussian-shaped pulse with  $T_{\text{FWHM}} = 10 \sqrt{\ln 2}$  ps and an amplitude of 0.07 V is used as the modulation signal that superimposes on a dc bias level of 1.2 V. Without any load termination, the output optical pulse profile shows multiple reflection structures that come from the interfaces between the optical waveguide and the feed line, and between the feed lines and the source/load. These reflections have the same sign as the output signal because both the source and the load have higher impedance than the waveguide (characteristic impedance  $\sim 25 \Omega$ ) and the feed line (characteristic impedance  $\sim 42 \Omega$ ). The reflections become much weaker when a 50- $\Omega$  termination is used. The reflection changes the sign when the load impedance is reduced to 32  $\Omega$  and cancels the reflection at the connections between the optical waveguide and the feed lines. This cancellation in reflection causes a frequency response enhancement at high frequencies. This is another proof that the device is operating in a traveling-wave mode. The inductance due to the ribbon is about 0.07 nH and is not the main reason for this resonance as verified by simulation. The use of a 32- $\Omega$  load will increase the required drive voltage, which is about 1.2 times that required for a load of 50  $\Omega$ . This could be overcome by the longer device length than that of conventional EA modulators.

To separate the microwave propagation loss from the impedance-mismatch induced reflection loss, the microwave transmission ( $S_{21}$ ) for devices with lengths of 300, 400,

500, and 600  $\mu\text{m}$  was measured. It is found that at 20 GHz, the 600- $\mu\text{m}$  devices have about 2.0-dB extra loss than 300- $\mu\text{m}$  devices. This suggests that for the 300- $\mu\text{m}$  device, the propagation loss at 20 GHz is about 2.0 dB, while the sum of the reflection loss and the other excess loss is about 1.0 dB since the total microwave loss is 3.0 dB. Consequently, to improve the device bandwidth, we need to reduce the propagation loss and increase the waveguide characteristic impedance to reduce the reflection loss.

The improvement in bandwidth with terminating the transmission line is larger for longer devices, as expected for a traveling-wave modulator. However, the propagation loss (about 0.67 dB/100  $\mu\text{m}$  at 20 GHz) is the dominant factor that limits the bandwidth in longer devices.

Long distance digital transmission has been demonstrated at 10 and 30 Gb/s with the 300- $\mu\text{m}$  traveling-wave modulator and will be presented in the future.

## V. CONCLUSION

We have demonstrated traveling-wave electroabsorption modulators using the InGaAsP–InGaAsP–InP material system. For a 300- $\mu\text{m}$ -long device, a modulation bandwidth of 25 GHz is achieved. The devices show little dependence on the polarization state. Driving voltages of 1.20 and 1.28 V are achieved for an extinction ratio of 20 dB for TE and TM modes. A resonance effect is observed for devices terminated with 32- $\Omega$  loads. This resonance effect is the result of microwave reflections at the source and the load ends. These results show that with good design, traveling-wave EA modulators can overcome the RC limitation and obtain higher

speed, lower driving voltage and larger extinction ratio for optical fiber communication applications.

## ACKNOWLEDGMENT

The authors would like to thank L. Coldren, E. Hu, N. Dagli, V. Kaman, S. Fleischer, T. Liljeberg, B. Mason, and G. Fish for valuable discussions.

## REFERENCES

- [1] F. Devaux and A. Carengo, "Optical processing with electroabsorption modulators," in *OFC'98 Tech. Dig.*, 1998, pp. 285–287, paper ThH3.
- [2] F. Devaux, S. Chelles, A. Ougazzaden, A. Mircea, and J. C. Harmand, "Electroabsorption modulators for high-bit-rate optical communications: A comparison of strained InGaAs/InAlAs and InGaAsP/InGaAsP MQW," *Semiconduct. Sci. Technol.*, vol. 10, pp. 887–901, 1995.
- [3] T. Ido, S. Tanaka, M. Suzuki, M. Koizumi, H. Sano, and H. Inoue, "Ultra-high-speed multiple-quantum-well electro-absorption optical modulators with integrated waveguides," *J. Lightwave Technol.*, vol. 14, pp. 2026–2034, 1996.
- [4] K. Wakita, K. Yoshino, I. Kotaka, S. Kondo, and Y. Noguchi, "High-speed, high efficiency modulator with polarization insensitive and very low chirp," *Electron. Lett.*, vol. 31, pp. 2041–2042, 1995.
- [5] K. Kawano, M. Kohtoku, M. Ueki, T. Ito, S. Kondoh, Y. Noguchi, and Y. Hasumi, "Polarization-insensitive travelling-wave electrode electroabsorption (TW-EA) modulator with bandwidth over 50 GHz and driving voltage less than 2 V," *Electron. Lett.*, vol. 33, pp. 1580–1581, 1997.
- [6] H. Liao, X. Mei, K. Loi, and C. Tu, "Microwave structures for traveling-wave MQW electro-absorption modulators for wide band 1.3  $\mu\text{m}$  photonic links," *Proc. SPIE*, vol. 3006, pp. 291–300, 1997.
- [7] S. Zhang, Y. Chiu, P. Abraham, and J. Bowers, "Polarization-insensitive multiple-quantum-well traveling-wave electroabsorption modulators with 18 GHz bandwidth and 1.2 V driving voltage at 1.55  $\mu\text{m}$ ," in *Int. Topical Meeting Microwave Photonics (MWP'98)*, Princeton, NJ, Oct., 1998, pp. 33–36, paper MC2.
- [8] K. Giboney, M. Rodwell, and J. Bowers, "Traveling-wave photodetector theory," *IEEE Trans. Microwave Theory Tech.*, vol. 45, pp. 1310–1319, 1997.